

Electromagnetic scattering by optically anisotropic magnetic particleZhifang Lin^{1,2} and S. T. Chui²¹*Surface Physics Laboratory, Research Center of Theoretical Physics, Department of Physics, Fudan University, Shanghai 200433, China*²*Bartol Research Institute, University of Delaware, Newark, Delaware 19716, USA*

(Received 8 December 2003; published 28 May 2004)

The Mie theory for electromagnetic scattering by spherical particle is extended to the case of magnetic particle with gyromagnetic type of permeability. Specifically, we first construct for the magnetic induction \mathbf{B}_l inside the particle a new set of vector basis functions, which are the solution of the wave equation for \mathbf{B}_l and expanded in terms of the usual vector spherical wave functions (VSWF's) with different values of wave vector k_l . The relationship between k_l and the frequency is obtained as the eigenvalues of an eigensystem determined by the permeability tensor. The incident and scattered fields are expanded as usual in terms of the VSWF's. By matching the boundary conditions, a linear set of coupled equations for the expansion coefficients are obtained and then solved for the solution to the scattering problem. Preliminary numerical results are presented for the case in which the scattering is due solely to the optical anisotropy within the particle. The scattering efficiency is found to exhibit miscellaneous dependence on the incident angle, the polarization, the degree of anisotropy, as well as the size parameter. In addition, the possibility of the photonic Hall effect for one Mie scatterer is confirmed.

DOI: 10.1103/PhysRevE.69.056614

PACS number(s): 42.25.Bs, 42.25.Fx, 52.25.Tx

I. INTRODUCTION

The purpose of this paper is to present a Mie-type solution to the problem of the scattering of plane electromagnetic (EM) waves by a magnetic sphere of arbitrary size and with gyromagnetic permeability tensor $\vec{\mu}$,

$$\vec{\mu} = \mu_s \begin{pmatrix} \mu_r & -i\mu_\kappa & 0 \\ i\mu_\kappa & \mu_r & 0 \\ 0 & 0 & 1 \end{pmatrix}, \quad (1)$$

for arbitrary directions of propagation and polarization of the incident plane waves. The research is motivated by the following aspects. First, much experimental and theoretical efforts have been recently devoted to the study of negative refractive index materials (NIM's, also known as left-handed materials) [1–6]. These metamaterials are characterized by simultaneously negative electric permittivity and magnetic permeability and are thus expected to possess unusual electromagnetic effects such as subwavelength focusing [1,3]. The first successful fabrication of the NIM's is the so-called “split-ring wire” structure [2]. One of us has proposed an alternative possibility of making the NIM's based on metallic magnetic granular composites. Based on the effective medium approximation, it was shown that by incorporating metallic magnetic nanoparticles into an appropriate insulating matrix, and controlling the directions of magnetization of metallic magnetic components and their volume fraction, it may be possible to prepare a composite medium of low eddy current loss which is left handed for electromagnetic waves propagating in some special direction and polarization in a frequency region near the ferromagnetic resonance frequency [7,8]. Further exploring the possibility beyond the effective medium approximation requires a more exact formalism of EM scattering that takes into account the anisotropic charac-

teristics (1) of the magnetic particles near the ferromagnetic resonance frequency.

Second, another class of artificial metamaterials that have received an increasing amount of interest is the photonic crystals, which has a characteristic size of spatial inhomogeneity that is comparable to the wavelength. Due partly to the lack of efficient methods, however, little attention has been paid to periodic structures composed of magnetic particles, which can be a photonic band-gap material tunable by magnetic field and temperature [9]. Actually, most calculations for photonic crystals composed of optically anisotropic materials are based on plane-wave expansion method, which can sometimes suffer from large errors and nonconvergence, especially when modeling systems with sharp contrast of material parameters or complex lattice structure [10].

Third, many experiments have been done with manipulating light with a magnetic field [11] as well as the diffusion of light in a magnetic field [12–17]. Up to now, theories that take into account the anisotropy of the optical parameters use pointlike scatterers [18,19] or are based on a perturbational approach [20,21]. Although the perturbation approach seems quite successful for the case of magnetoactive particles for which the anisotropy induced by magnetic field is rather small, it may not produce correct results for the case of ferrite or other magnetic particles where one may expect much greater anisotropic changes induced by the magnetic field.

Fourth, composites with magnetic particles may be used as microwave filters. The first step in understanding this possibility requires the basic knowledge discussed here.

Finally, multiple radiative scattering by particles is a common subject in a wide range of scientific and technical fields stretching from astrophysics, climatology, nanoscience, remote sensing to aerosol medicine [22]. Two of the most powerful and widely used tools for rigorously computing multiparticle scattering are the cluster T matrix approach [23] and the generalized multiparticle Mie solution [24], both requir-

ing the computation of the proper T matrix of a single particle. Although many efficient approaches have been proposed for evaluating the proper T matrix of geometrically anisotropic particle [23], little attention has been paid to the optically anisotropic scatterer [25].

As a result, it is desirable to have a generalized Mie-type formulation for EM scattering with anisotropic permeability (or permittivity) of the form such as Eq. (1), which serves as the building block for all the above multiple scattering problems.

The rest of the paper is organized as follows. In Sec. II, we present a comprehensive derivation of a Mie-type solution to the problem of the scattering of plane EM waves by an optically anisotropic magnetic particle. In Sec. III, we make some brief comments on the numerical strategy and present some numerical results. A summary is given in Sec. IV. Details on some technical results are relegated to the appendices.

II. GENERAL FORMULATION

We start in Sec. II A by constructing for the magnetic induction \mathbf{B}_I inside the anisotropic sphere a new set of vector basis functions, each of which is the solution of the wave equation for \mathbf{B}_I and expanded in terms of the usual vector spherical wave functions (VSWF's) with the values of the wave vector k_I obtained as the eigenvalues of an eigensystem determined by permeability tensor. The electric and magnetic fields are then written as sums of the VSWF's with the different values of k_I . After expanding the incident and scattered fields in terms of VSWF's in the isotropic medium outside the sphere in Sec. II B, we match the boundary conditions to obtain a linear set of coupled equations for the expansion coefficients in Sec. II C. Expressions for evaluating scattering properties such as scattering and extinction efficiency based on the expansion coefficients are given in Sec. II D.

A. Expansion of electromagnetic field inside sphere

The Maxwell equations for time-harmonic field inside the sourceless and homogeneous sphere read (assuming time dependence $e^{-i\omega t}$),

$$\nabla \times \mathbf{E}_I = i\omega \mathbf{B}_I, \quad (2a)$$

$$\nabla \times \mathbf{H}_I = -i\omega \mathbf{D}_I \quad (2b)$$

$$\nabla \cdot \mathbf{D}_I = 0, \quad (2c)$$

$$\nabla \cdot \mathbf{B}_I = 0. \quad (2d)$$

The constitutive relations between the electric displacement vector \mathbf{D}_I , the magnetic induction \mathbf{B}_I , the electric field \mathbf{E}_I , and the magnetic field \mathbf{H}_I inside the particle are given by

$$\mathbf{B}_I = \vec{\mu} \cdot \mathbf{H}_I, \quad \mathbf{D}_I = \epsilon_s \mathbf{E}_I, \quad (3)$$

where the permeability tensor $\vec{\mu}$ is given by Eq. (1), and ϵ_s is the scalar permittivity. It follows from Eq. (2) that the \mathbf{B} field inside the particle satisfies the wave equation

$$\nabla \times \nabla \times (\mu_s \vec{\mu}^{-1} \cdot \mathbf{B}_I) - k_s^2 \mathbf{B}_I = 0 \quad (4)$$

with $k_s^2 = \omega^2 \epsilon_s \mu_s$ and

$$\mu_s \vec{\mu}^{-1} = \begin{pmatrix} \mu'_r & -i\mu'_\kappa & 0 \\ i\mu'_\kappa & \mu'_r & 0 \\ 0 & 0 & 1 \end{pmatrix}, \quad (5)$$

where

$$\mu'_r = \frac{\mu_r}{\mu_r^2 - \mu_\kappa^2}, \quad \mu'_\kappa = -\frac{\mu_\kappa}{\mu_r^2 - \mu_\kappa^2}. \quad (6)$$

The divergenceless property (2d) suggests that \mathbf{B}_I be expanded in terms of the vector spherical wave functions $\mathbf{M}_{mn}^{(1)}(k, \mathbf{r})$ and $\mathbf{N}_{mn}^{(1)}(k, \mathbf{r})$ [26]

$$\mathbf{B}_I = \sum_{n,m} \bar{E}_{mn} [d_{mn} \mathbf{M}_{mn}^{(1)}(k, \mathbf{r}) + c_{mn} \mathbf{N}_{mn}^{(1)}(k, \mathbf{r})], \quad (7)$$

where k is as yet undetermined. In general, there are three kinds of VSWF's $\mathbf{M}_{mn}^{(J)}(k, \mathbf{r})$, $\mathbf{N}_{mn}^{(J)}(k, \mathbf{r})$, and $\mathbf{L}_{mn}^{(J)}(k, \mathbf{r})$. The divergenceless property of \mathbf{B} implies that it does not involve \mathbf{L}_{mn} , thereby simplifying the algebra involved. The three kinds of VSWF's are given for $J=1$ and 3 in Appendix A. Except otherwise explicitly specified, hereinafter the summation $\sum_{n,m}$ implies that n runs from 1 to $+\infty$ and m from $-n$ to $+n$ for each n . The implication of $\sum_{v,u}$ is similar. The prefactor $\bar{E}_{mn} = i^n E_0 C_{mn}$ with [24]

$$C_{mn} = \left[\frac{2n+1}{n(n+1)} \frac{(n-m)!}{(n+m)!} \right]^{1/2}, \quad (8)$$

where E_0 characterizes the amplitude of electric field of the incident wave. With the use of the properties of VSWF's, it can be worked out that (see Appendix B)

$$\begin{aligned} \mu_s \vec{\mu}^{-1} \cdot \mathbf{M}_{mn} &= \sum_{v=0}^{+\infty} \sum_{u=-v}^{+v} [\tilde{g}_{uv}^{mn} \mathbf{M}_{uv} + \tilde{e}_{uv}^{mn} \mathbf{N}_{uv} + \tilde{f}_{uv}^{mn} \mathbf{L}_{uv}], \\ \mu_s \vec{\mu}^{-1} \cdot \mathbf{N}_{mn} &= \sum_{v=0}^{+\infty} \sum_{u=-v}^{+v} [\tilde{g}_{uv}^{mn} \mathbf{M}_{uv} + \tilde{e}_{uv}^{mn} \mathbf{N}_{uv} + \tilde{f}_{uv}^{mn} \mathbf{L}_{uv}], \end{aligned} \quad (9)$$

where, with $\bar{\mu}'_r = \mu'_r - 1$,

$$\tilde{g}_{uv}^{mn} = \delta_{nv} \delta_{mu} + \frac{[(n^2 + n - m^2) \bar{\mu}'_r + m \mu'_\kappa] \delta_{nv} \delta_{mu}}{n(n+1)}, \quad (10a)$$

$$\begin{aligned} \tilde{e}_{uv}^{mn} &= \frac{i(n+m)[m \bar{\mu}'_r - (n+1) \mu'_\kappa] \delta_{n-1,v} \delta_{mu}}{n(2n+1)} \\ &+ \frac{i(n-m+1)[m \bar{\mu}'_r + n \mu'_\kappa] \delta_{n+1,v} \delta_{mu}}{(n+1)(2n+1)}, \end{aligned} \quad (10b)$$

$$\begin{aligned} \tilde{f}_{uv}^{mn} = & \frac{-i(n+m)[m\bar{\mu}'_r - (n+1)\mu'_\kappa]\delta_{n-1,v}\delta_{mu}}{(2n+1)} \\ & + \frac{i(n-m+1)[m\bar{\mu}'_r + n\mu'_\kappa]\delta_{n+1,v}\delta_{mu}}{(2n+1)}, \end{aligned} \quad (10c)$$

$$\begin{aligned} \bar{g}_{uv}^{mn} = & -\frac{i(n+m)(n+1)[m\bar{\mu}'_r + (n-1)\mu'_\kappa]\delta_{n-1,v}\delta_{mu}}{n(n-1)(2n+1)} \\ & - \frac{i(n-m+1)n[m\bar{\mu}'_r - (n+2)\mu'_\kappa]\delta_{n+1,v}\delta_{mu}}{(n+1)(n+2)(2n+1)}, \end{aligned} \quad (10d)$$

$$\begin{aligned} \bar{e}_{uv}^{mn} = & \delta_{nv}\delta_{mu} + \frac{\{[(2n^2+2n+3)m^2 + (2n^2+2n-3)n(n+1)]\bar{\mu}'_r + (4n^2+4n-3)m\mu'_\kappa\}\delta_{nv}\delta_{mu}}{n(n+1)(2n-1)(2n+3)} \\ & - \frac{(n+1)(n+m-1)(n+m)\bar{\mu}'_r\delta_{n-2,v}\delta_{mu}}{(n-1)(2n-1)(2n+1)} - \frac{n(n-m+1)(n-m+2)\bar{\mu}'_r\delta_{n+2,v}\delta_{mu}}{(n+2)(2n+1)(2n+3)}, \end{aligned} \quad (10e)$$

$$\begin{aligned} \bar{f}_{uv}^{mn} = & -\frac{[(n^2+n-3m^2)\bar{\mu}'_r - m(2n-1)(2n+3)\mu'_\kappa]\delta_{nv}\delta_{mu}}{(2n-1)(2n+3)} \\ & + \frac{(n+1)(n+m-1)(n+m)\bar{\mu}'_r\delta_{n-2,v}\delta_{mu}}{(2n-1)(2n+1)} \\ & - \frac{n(n-m+1)(n-m+2)\bar{\mu}'_r\delta_{n+2,v}\delta_{mu}}{(2n+1)(2n+3)}. \end{aligned} \quad (10f)$$

Therefore, one has

$$\begin{aligned} \mu_s \bar{\mu}^{-1} \cdot \mathbf{B}_l = & \sum_{n,m} \bar{E}_{mn} [\bar{d}_{mn} \mathbf{M}_{mn}^{(1)}(k, \mathbf{r}) + \bar{c}_{mn} \mathbf{N}_{mn}^{(1)}(k, \mathbf{r}) \\ & + w_{mn} \mathbf{L}_{mn}^{(1)}(k, \mathbf{r})] + w_{00} \mathbf{L}_{00}^{(1)}(k, \mathbf{r}), \end{aligned} \quad (11)$$

where

$$\bar{d}_{mn} = \sum_{v,u} \frac{\bar{E}_{uv}}{\bar{E}_{mn}} [\bar{g}_{mn}^{uv} d_{uv} + \bar{g}_{mn}^{uv} c_{uv}], \quad (12a)$$

$$\bar{c}_{mn} = \sum_{v,u} \frac{\bar{E}_{uv}}{\bar{E}_{mn}} [\bar{e}_{mn}^{uv} d_{uv} + \bar{e}_{mn}^{uv} c_{uv}], \quad (12b)$$

$$w_{mn} = \sum_{v,u} \frac{\bar{E}_{uv}}{\bar{E}_{mn}} [\tilde{f}_{mn}^{uv} d_{uv} + \tilde{f}_{mn}^{uv} c_{uv}], \quad (12c)$$

$$w_{00} = -\sqrt{\frac{2}{3}} \mu'_\kappa d_{01} - \sqrt{\frac{2}{15}} \bar{\mu}'_r c_{02}. \quad (12d)$$

Inserting Eqs. (7) and (11) into the wave equation (4), and noticing the following equations satisfied by the VSWF's

$$\nabla \times \nabla \times \mathbf{M}_{mn}^{(1)} - k^2 \mathbf{M}_{mn}^{(1)} = 0,$$

$$\nabla \times \nabla \times \mathbf{N}_{mn}^{(1)} - k^2 \mathbf{N}_{mn}^{(1)} = 0,$$

$$\nabla \times \mathbf{L}_{mn}^{(1)} = 0 \quad (13)$$

one gets

$$\sum_{n,m} \bar{E}_{mn} [\bar{d}_{mn} \mathbf{M}_{mn}^{(1)}(k, \mathbf{r}) + \bar{c}_{mn} \mathbf{N}_{mn}^{(1)}(k, \mathbf{r})] = 0, \quad (14)$$

with

$$\begin{aligned} \bar{d}_{mn} = & k^2 \sum_{v,u} \frac{\bar{E}_{uv}}{\bar{E}_{mn}} [\bar{g}_{mn}^{uv} d_{uv} + \bar{g}_{mn}^{uv} c_{uv}] - k_s^2 d_{mn}, \\ \bar{c}_{mn} = & k^2 \sum_{v,u} \frac{\bar{E}_{uv}}{\bar{E}_{mn}} [\bar{e}_{mn}^{uv} d_{uv} + \bar{e}_{mn}^{uv} c_{uv}] - k_s^2 c_{mn}. \end{aligned} \quad (15)$$

Equations (14) and (15) imply an eigensystem governing the value of k for expansion (7),

$$\begin{pmatrix} \bar{\mathcal{G}} & \bar{\mathcal{G}} \\ \bar{\mathcal{E}} & \bar{\mathcal{E}} \end{pmatrix} \begin{pmatrix} d \\ c \end{pmatrix} = \lambda \begin{pmatrix} d \\ c \end{pmatrix}, \quad (16)$$

where $\lambda = k_s^2/k^2$, and the matrices $\bar{\mathcal{G}}$, $\bar{\mathcal{G}}$, $\bar{\mathcal{E}}$, and $\bar{\mathcal{E}}$ are given by

$$\begin{aligned} \bar{\mathcal{G}}_{mn,uv} = & \frac{\bar{E}_{uv}}{\bar{E}_{mn}} \bar{g}_{mn}^{uv}, & \bar{\mathcal{G}}_{mn,uv} = & \frac{\bar{E}_{uv}}{\bar{E}_{mn}} \bar{g}_{mn}^{uv}, \\ \bar{\mathcal{E}}_{mn,uv} = & \frac{\bar{E}_{uv}}{\bar{E}_{mn}} \bar{e}_{mn}^{uv}, & \bar{\mathcal{E}}_{mn,uv} = & \frac{\bar{E}_{uv}}{\bar{E}_{mn}} \bar{e}_{mn}^{uv}, \end{aligned} \quad (17)$$

with mn and uv denoting the row and column indices, respectively. Let λ_l and $(d_{mn,l}, c_{mn,l})^T$ denote, respectively, the eigenvalues and the corresponding eigenvectors of eigensystem (16), with l representing the index of eigenvalues and corresponding eigenvectors. One can then construct a new set of vector functions \mathbf{V}_l based on the eigenvectors,

$$\mathbf{V}_l = -\frac{k_l}{\omega_{n,m}} \sum \bar{E}_{mn} [d_{mn,l} \mathbf{M}_{mn}^{(1)}(k_l, \mathbf{r}) + c_{mn,l} \mathbf{N}_{mn}^{(1)}(k_l, \mathbf{r})] \quad (18)$$

with $k_l = k_s / \sqrt{\lambda_l}$. It follows directly from

$$\nabla \cdot \mathbf{M}_{mn} = \nabla \cdot \mathbf{N}_{mn} = 0 \quad (19)$$

that \mathbf{V}_l are divergenceless

$$\nabla \cdot \mathbf{V}_l = 0. \quad (20a)$$

In addition, they satisfy the wave equation for \mathbf{B}_l field (4),

$$\nabla \times \nabla \times (\mu_s \tilde{\mu}^{-1} \cdot \mathbf{V}_l) - k_s^2 \mathbf{V}_l = 0. \quad (20b)$$

Thus, they form a new set of vector basis functions for \mathbf{B}_l , namely, \mathbf{B}_l can be expanded in terms of \mathbf{V}_l ,

$$\mathbf{B}_l = \sum_l \alpha_l \mathbf{V}_l, \quad (21)$$

where the expansion coefficients α_l are to be determined by matching the boundary conditions at the surface of sphere. With \mathbf{B}_l given by Eq. (21), it follows from Eqs. (2b) and (3) that \mathbf{H}_l and \mathbf{E}_l fields can be written as

$$\begin{aligned} \mathbf{H}_l &= \tilde{\mu}^{-1} \cdot \mathbf{B}_l \\ &= -\sum_{n,m} \bar{E}_{mn} \sum_l \frac{\omega \epsilon_s}{k_l} \alpha_l \left[d_{mn,l} \mathbf{M}_{mn}^{(1)}(k_l, \mathbf{r}) + c_{mn,l} \mathbf{N}_{mn}^{(1)}(k_l, \mathbf{r}) \right. \\ &\quad \left. + \frac{w_{mn,l}}{\lambda_l} \mathbf{L}_{mn}^{(1)}(k_l, \mathbf{r}) \right] + \sum_l \frac{\omega \epsilon_s}{k_l} \alpha_l \left[\frac{w_{00,l}}{\lambda_l} \mathbf{L}_{00}^{(1)}(k_l, \mathbf{r}) \right], \end{aligned} \quad (22a)$$

$$\begin{aligned} \mathbf{E}_l &= \frac{i}{\omega \epsilon_s} \nabla \times \mathbf{H}_l \\ &= -\sum_{n,m} i \bar{E}_{mn} \sum_l \alpha_l [c_{mn,l} \mathbf{M}_{mn}^{(1)}(k_l, \mathbf{r}) + d_{mn,l} \mathbf{N}_{mn}^{(1)}(k_l, \mathbf{r})] \end{aligned} \quad (22b)$$

where use has been made of Eqs. (11), (12), and (15), whereas

$$w_{mn,l} = \sum_{v,u} \frac{\bar{E}_{uv}}{\bar{E}_{mn}} [\tilde{f}_{mn}^{uv} d_{uv,l} + \bar{f}_{mn}^{uv} c_{uv,l}], \quad (23a)$$

$$w_{00,l} = -\sqrt{\frac{2}{3}} \mu'_r d_{01,l} - \sqrt{\frac{2}{15}} \bar{\mu}'_r c_{02,l}. \quad (23b)$$

Notice that, since $\nabla \cdot \mathbf{H}_l \neq 0$, its expansion includes \mathbf{L}_{mn} terms that are absent in the isotropic case.

B. Expansion of the scattered and incident fields

The scattered fields \mathbf{E}_s , \mathbf{H}_s , and incident fields \mathbf{E}_{inc} , \mathbf{H}_{inc} in the isotropic surrounding medium have the same form as in Mie solution [26,27]. Notice, however, that the form of the permeability tensor (1) we have used implies that the magnetization direction of the magnetic particle is along the z axis. For arbitrary directions of propagation and polarization of the incident plane waves, the expansions of the field are not limited to $m = \pm 1$ modes.

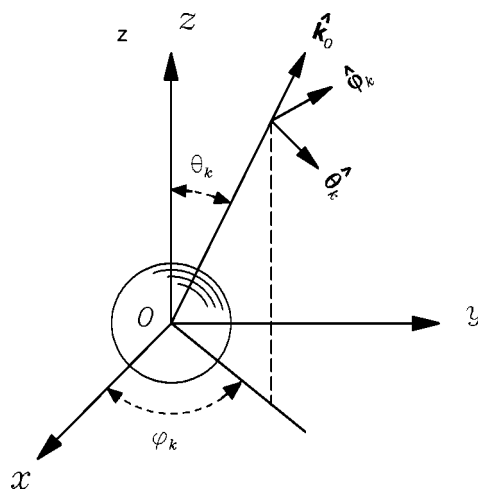


FIG. 1. Geometry of the scattering problem.

In terms of VSWF's, the scattered fields ($\mathbf{E}_s, \mathbf{H}_s$) are expanded as

$$\begin{aligned} \mathbf{E}_s &= \sum_{n,m} i \bar{E}_{mn} [a_{mn} \mathbf{N}_{mn}^{(3)}(k_0, \mathbf{r}) + b_{mn} \mathbf{M}_{mn}^{(3)}(k_0, \mathbf{r})], \\ \mathbf{H}_s &= \frac{k_0}{\omega \mu_{0,n,m}} \sum \bar{E}_{mn} [b_{mn} \mathbf{N}_{mn}^{(3)}(k_0, \mathbf{r}) + a_{mn} \mathbf{M}_{mn}^{(3)}(k_0, \mathbf{r})], \end{aligned} \quad (24)$$

where $k_0^2 = \omega^2 \epsilon_0 \mu_0$ with ϵ_0 and μ_0 being, respectively, the scalar permittivity and permeability of the surrounding medium. The expansion coefficients a_{mn} and b_{mn} are to be determined by matching boundary conditions.

Suppose that the particle is illuminated by a plane wave characterized by \mathbf{k}_0 , with

$$\mathbf{k}_0 = k_0 (\sin \theta_k \cos \phi_k \mathbf{e}_x + \sin \theta_k \sin \phi_k \mathbf{e}_y + \cos \theta_k \mathbf{e}_z), \quad (25)$$

where \mathbf{e}_x , \mathbf{e}_y , and \mathbf{e}_z are three unit base vectors of the Cartesian coordinate system and θ_k (ϕ_k) is the polar (azimuthal) angle of \mathbf{k}_0 , as shown in Fig. 1. The electric and magnetic fields of the incident plane wave are then

$$\begin{aligned} \mathbf{E}_{\text{inc}} &= E_0 (p_\theta \hat{\boldsymbol{\theta}}_k + p_\phi \hat{\boldsymbol{\phi}}_k) e^{i\mathbf{k}_0 \cdot \mathbf{r}}, \\ \mathbf{H}_{\text{inc}} &= \frac{k_0}{\omega \mu_0} E_0 (p_\theta \hat{\boldsymbol{\phi}}_k - p_\phi \hat{\boldsymbol{\theta}}_k) e^{i\mathbf{k}_0 \cdot \mathbf{r}}, \end{aligned} \quad (26)$$

where $\hat{\mathbf{p}} = (p_\theta \hat{\boldsymbol{\theta}}_k + p_\phi \hat{\boldsymbol{\phi}}_k)$ is the normalized complex polarization vector, with $|\hat{\mathbf{p}}| = 1$, and the unit vectors $\hat{\boldsymbol{\theta}}_k$ and $\hat{\boldsymbol{\phi}}_k$ are defined in the direction of increasing θ_k and ϕ_k such as to constitute a right-hand base system together with $\hat{\mathbf{k}}_0 = \mathbf{k}_0/k_0$, as shown in Fig. 1, namely,

$$\hat{\mathbf{k}}_0 \times \hat{\boldsymbol{\theta}}_k = \hat{\boldsymbol{\phi}}_k, \quad \hat{\boldsymbol{\theta}}_k \times \hat{\boldsymbol{\phi}}_k = \hat{\mathbf{k}}_0, \quad \hat{\boldsymbol{\phi}}_k \times \hat{\mathbf{k}}_0 = \hat{\boldsymbol{\theta}}_k. \quad (27)$$

With the use of the mathematical identity [28]

$$\vec{\mathbf{I}}e^{i\mathbf{k}_0 \cdot \mathbf{r}} = \sum_{n,m} [\mathbf{A}_{mn}\mathbf{N}_{mn}^{(1)}(k_0, \mathbf{r}) + \mathbf{B}_{mn}\mathbf{M}_{mn}^{(1)}(k_0, \mathbf{r}) + \mathbf{C}_{mn}\mathbf{L}_{mn}^{(1)}(k_0, \mathbf{r}) + \mathbf{C}_{00}\mathbf{L}_{00}^{(1)}(k_0, \mathbf{r})], \quad (28)$$

where $\vec{\mathbf{I}}$ is the unit dyad, and

$$\mathbf{A}_{mn} = \frac{2n+1}{n(n+1)} \frac{(n-m)!}{(n+m)!} i^{n-1} [-i\pi_{mn}(\cos \theta_k) \hat{\boldsymbol{\phi}}_k + \tau_{mn}(\cos \theta_k) \hat{\boldsymbol{\theta}}_k] e^{-im\phi_k},$$

$$\mathbf{B}_{mn} = \frac{2n+1}{n(n+1)} \frac{(n-m)!}{(n+m)!} i^n [-i\pi_{mn}(\cos \theta_k) \hat{\boldsymbol{\theta}}_k - \tau_{mn}(\cos \theta_k) \hat{\boldsymbol{\phi}}_k] e^{-im\phi_k},$$

$$\mathbf{C}_{mn} = (2n+1) \frac{(n-m)!}{(n+m)!} i^{n-1} P_n^m(\cos \theta_k) \hat{\mathbf{k}}_0 e^{-im\phi_k}, \quad \mathbf{C}_{00} = -i\mathbf{k}_0, \quad (29)$$

with $P_n^m(\cos \theta)$ the associated Legendre function of the first kind, the incident fields ($\mathbf{E}_{\text{inc}}, \mathbf{H}_{\text{inc}}$) can be expanded as

$$\mathbf{E}_{\text{inc}} = -\sum_{n,m} i\bar{E}_{mn} [p_{mn}\mathbf{N}_{mn}^{(1)}(k_0, \mathbf{r}) + q_{mn}\mathbf{M}_{mn}^{(1)}(k_0, \mathbf{r})],$$

$$\mathbf{H}_{\text{inc}} = -\frac{k_0}{\omega\mu_{0n,m}} \sum_{n,m} \bar{E}_{mn} [q_{mn}\mathbf{N}_{mn}^{(1)}(k_0, \mathbf{r}) + p_{mn}\mathbf{M}_{mn}^{(1)}(k_0, \mathbf{r})]. \quad (30)$$

The expansion coefficients p_{mn} and q_{mn} are

$$p_{mn} = [p_\theta \tilde{\tau}_{mn}(\cos \theta_k) - ip_\phi \tilde{\pi}_{mn}(\cos \theta_k)] e^{-im\phi_k}$$

$$q_{mn} = [p_\theta \tilde{\pi}_{mn}(\cos \theta_k) - ip_\phi \tilde{\tau}_{mn}(\cos \theta_k)] e^{-im\phi_k} \quad (31)$$

where the regular angular functions $\tilde{\pi}_{mn}(\cos \theta)$ and $\tilde{\tau}_{mn}(\cos \theta)$ are defined by [24]

$$\tilde{\pi}_{mn}(\cos \theta) = C_{mn} \frac{m}{\sin \theta} P_n^m(\cos \theta),$$

$$\tilde{\tau}_{mn}(\cos \theta) = C_{mn} \frac{d}{d\theta} P_n^m(\cos \theta), \quad (32)$$

with C_{mn} given by Eq. (8).

C. Matching boundary conditions

With the internal fields, scattered fields, and incident fields given, respectively, by Eqs. (22), (24), and (30), all expressed in terms of the usual VSWF's, one is ready to apply the standard boundary conditions

$$[\mathbf{E}_{\text{inc}} + \mathbf{E}_s] \times \mathbf{e}_r = \mathbf{E}_I \times \mathbf{e}_r,$$

$$[\mathbf{H}_{\text{inc}} + \mathbf{H}_s] \times \mathbf{e}_r = \mathbf{H}_I \times \mathbf{e}_r. \quad (33)$$

After some algebra, one gets the equations to determine the expansion coefficients α_l , a_{mn} , and b_{mn} , based on p_{mn} and q_{mn} ,

$$\left[\frac{\xi'_n(x)}{\psi'_n(x)} \right] a_{mn} + \sum_l \left[\frac{1}{m_s \bar{k}_l} \frac{\psi'_n(\bar{k}_l m_s x)}{\psi'_n(x)} d_{mn,l} \right] \alpha_l = p_{mn}, \quad (34a)$$

$$\left[\frac{\xi_n(x)}{\psi_n(x)} \right] b_{mn} + \sum_l \left[\frac{1}{m_s \bar{k}_l} \frac{\psi_n(\bar{k}_l m_s x)}{\psi_n(x)} c_{mn,l} \right] \alpha_l = q_{mn}, \quad (34b)$$

$$\left[\frac{\xi_n(x)}{\psi_n(x)} \right] a_{mn} + \sum_l \left[\frac{\mu_0 \lambda_l}{\mu_s} \frac{\psi_n(\bar{k}_l m_s x)}{\psi_n(x)} d_{mn,l} \right] \alpha_l = p_{mn}, \quad (34c)$$

$$\left[\frac{\xi'_n(x)}{\psi'_n(x)} \right] b_{mn} + \sum_l \left[\frac{\mu_0 \lambda_l}{\mu_s} \frac{\psi'_n(\bar{k}_l m_s x)}{\psi'_n(x)} c_{mn,l} \right] \alpha_l$$

$$+ \sum_l \left[\frac{\mu_0 j_n(\bar{k}_l m_s x)}{\mu_s} w_{mn,l} \right] \alpha_l = q_{mn}, \quad (34d)$$

where the size parameter $x = k_0 r_s$, with r_s the radius of sphere, and

$$m_s = \frac{k_s}{k_0}, \quad \bar{k}_l = \frac{k_l}{k_s}.$$

$$k_l = m_s \bar{k}_l k_0, \quad \lambda_l = \frac{k_l^2}{k_l^2} = \frac{1}{k_l^2}. \quad (35)$$

The Riccati-Bessel functions $\psi_n(z)$ and $\xi_n(z)$ are given by [27]

$$\psi_n(z) = z j_n(z), \quad \xi_n(z) = z h_n^{(1)}(z), \quad (36)$$

with $j_n(z)$ and $h_n^{(1)}(z)$ being, respectively, the spherical Bessel functions of the first and third kinds. The last term on the left-hand side of Eq. (34d) originates from the \mathbf{L}_{mn} terms in the expansion of \mathbf{H}_I field (22). Equations (34) can be rewritten in matrix form

$$\begin{pmatrix} \bar{\Lambda} & 0 \\ 0 & \Lambda \end{pmatrix} \begin{pmatrix} a \\ b \end{pmatrix} + \begin{pmatrix} \bar{U} \\ U \end{pmatrix} \tilde{\alpha} = \begin{pmatrix} p \\ q \end{pmatrix}, \quad (37a)$$

$$\begin{pmatrix} \Lambda & 0 \\ 0 & \bar{\Lambda} \end{pmatrix} \begin{pmatrix} a \\ b \end{pmatrix} + \begin{pmatrix} V \\ \bar{V} \end{pmatrix} \tilde{\alpha} = \begin{pmatrix} p \\ q \end{pmatrix}. \quad (37b)$$

The matrices are given by

$$\Lambda_{mn,uv} = S_n(x) \delta_{nv} \delta_{mu},$$

$$\bar{\Lambda}_{mn,uv} = \bar{S}_n(x) \delta_{nv} \delta_{mu},$$

$$U_{mn,l} = \frac{1}{m_s \bar{k}_l} T_n(x, m_s \bar{k}_l x) c_{mn,l},$$

$$\bar{U}_{mn,l} = \frac{1}{m_s \bar{k}_l} \bar{T}_n(x, m_s \bar{k}_l x) d_{mn,l},$$

$$V_{mn,l} = \frac{\mu_0 \lambda_l}{\mu_s} T_n(x, m_s \bar{k}_l x) d_{mn,l},$$

$$\bar{V}_{mn,l} = \frac{\mu_0 \lambda_l}{\mu_s} \bar{T}_n(x, m_s \bar{k}_l x) c_{mn,l} + W_{mn,l},$$

$$W_{mn,l} = \frac{\mu_0}{\mu_s} \frac{1}{m_s \bar{k}_l x} \frac{\bar{T}_n(x, m_s \bar{k}_l x)}{D_n^{(1)}(m_s \bar{k}_l x)} w_{mn,l}, \quad (38)$$

where

$$S_n(x) = \frac{\xi_n(x)}{\psi_n(x)}, \quad \bar{S}_n(x) = \frac{\xi'_n(x)}{\psi'_n(x)},$$

$$T_n(x, z) = \frac{\psi_n(z)}{\psi_n(x)}, \quad \bar{T}_n(x, z) = \frac{\psi'_n(z)}{\psi'_n(x)}, \quad (39)$$

and the logarithmic derivatives of the Riccati-Bessel function

$$D_n^{(1)}(z) = \frac{\psi'_n(z)}{\psi_n(z)}.$$

Equations (37a) and (37b) can be solved to give

$$\bar{\alpha} = \mathcal{R} \begin{pmatrix} p \\ q \end{pmatrix} \quad (40a)$$

$$\begin{pmatrix} a \\ b \end{pmatrix} = \mathcal{S} \begin{pmatrix} p \\ q \end{pmatrix} \quad (40b)$$

where

$$\mathcal{R} = \left[\begin{pmatrix} \bar{U} \\ U \end{pmatrix} + \begin{pmatrix} \bar{\Lambda} & 0 \\ 0 & \Lambda \end{pmatrix} \mathcal{Z} \right]^{-1}, \quad (41a)$$

$$\mathcal{Z} = \begin{pmatrix} Y & 0 \\ 0 & -Y \end{pmatrix}^{-1} \begin{pmatrix} V - \bar{U} \\ \bar{V} - U \end{pmatrix}, \quad (41b)$$

$$\mathcal{S} = \mathcal{Z} \mathcal{R}, \quad (41c)$$

$$Y = \bar{\Lambda} - \Lambda. \quad (41d)$$

D. Scattering properties

With the expansion coefficients a_{mn} and b_{mn} that characterize the scattered fields obtained from Eq. (40b), it is straightforward to evaluate fields outside the particle as a sum of the scattered fields (24) and the incident fields (30).

The efficiency factors for scattering Q_{sca} , extinction Q_{ext} , and absorption Q_{abs} , as well as the asymmetry parameter $g = \langle \cos \theta \rangle$ [27] can be expressed based on a_{mn} and b_{mn} . The only difference from the Mie theory is that one should include all terms instead of only the $m = \pm 1$ terms. Explicitly, they are given by [24]

$$Q_{\text{sca}} = \frac{4}{x^2} \sum_{n,m} (|a_{mn}|^2 + |b_{mn}|^2), \quad (42a)$$

$$Q_{\text{ext}} = \frac{4}{x^2} \sum_{n,m} \text{Re}(p_{mn}^* a_{mn} + q_{mn}^* b_{mn}), \quad (42b)$$

$$Q_{\text{abs}} = Q_{\text{ext}} - Q_{\text{sca}}, \quad (42c)$$

$$g = \frac{4}{x^2 Q_{\text{sca},n,m}} \sum \text{Re}(a_{mn}^* \tilde{a}_{mn} + b_{mn}^* \tilde{b}_{mn}), \quad (42d)$$

where the superscript * stands for the complex conjugate, and

$$\tilde{a}_{mn} = f_1 b_{mn} + f_2 a_{mn+1} + f_3 a_{mn-1},$$

$$\tilde{b}_{mn} = f_1 a_{mn} + f_2 b_{mn+1} + f_3 b_{mn-1}, \quad (43)$$

with

$$f_1 = \frac{m}{n(n+1)},$$

$$f_2 = \frac{1}{n+1} \left[\frac{n(n+2)(n-m+1)(n+m+1)}{(2n+1)(2n+3)} \right]^{1/2},$$

$$f_3 = \frac{1}{n} \left[\frac{(n-1)(n+1)(n-m)(n+m)}{(2n-1)(2n+1)} \right]^{1/2}. \quad (44)$$

The fields inside the particle are evaluated based on Eq. (22), with α_l given by Eq. (40a).

III. NUMERICAL RESULTS

The general formulation in the preceding section applies, in principle, to the case with arbitrarily anisotropic permeability, provided that the expansion coefficients of $\vec{\mu}^{-1} \cdot \mathbf{M}_{mn}$ and $\vec{\mu}^{-1} \cdot \mathbf{N}_{mn}$ in terms of VSWF's such as Eq. (9) can be worked out. In Sec. III A, we exploit the axial symmetry of the permeability tensor to simplify the eigensystem (16) and the linear system (37). Algorithms for computing some variables appearing in matrix elements are described in Sec. III B. In Sec. III C, we present some numerical results that demonstrate the effect due solely to optical anisotropy on scattering properties. In Sec. III D, we address the issue of the magnetotransverse anisotropy in light scattering, the so-called photonic Hall effect, for a single Mie scatterer.

A. Simplification of the eigensystem and the linear system

As in Mie scattering, in practical calculation, the series expansion of Eq. (22) is supposed to be uniformly conver-

gent and can be truncated at some $n=n_c$. The resultant error incurred due to truncation is assumed to be insignificant. The criterion for the determination of the required scattering terms for Mie scattering is well established [27,29], which is

$$n_c = x + 4x^{1/3} + 2, \quad (45)$$

where $x=k_0r_s$ is the size parameter. In the present case, the value of n_c depends also on degree of anisotropy, usually requiring a greater value of n_c for a greater anisotropy.

If one terminates the series expansion at some degree $n=n_c$ and adopts the usual combined index j to represent the two indices mn [28]

$$j = n(n+1) + m, \quad (46)$$

then $\tilde{\mathcal{G}}, \bar{\mathcal{G}}, \tilde{\mathcal{E}},$ and $\bar{\mathcal{E}}$ in the eigensystem (16) are all $n_d \times n_d$ matrices, with $n_d=n_c(n_c+2)$, while in the linear system (37), Λ and $\bar{\Lambda}$ are $n_d \times n_d$ diagonal matrices, $U, \bar{U}, V, \bar{V},$ and W are $n_d \times n_t$ matrices, while $\tilde{\alpha}$ is a $n_t \times 1$ matrix. Here $n_t=2n_d$. The solution requires computing the inverse of $n_t \times n_t$ matrices as shown in Eq. (41a)–(41d), as well as calculating all eigenvalues and eigenvectors of an $n_t \times n_t$ matrix (16).

The axial symmetry of permeability (1) suggests two characteristics that, corresponding to two Kronecker δ symbols in Eq. (10), may greatly simplify the calculation. The first Kronecker symbol δ_{mu} indicates that one may solve for the eigensystem (16) and linear system (37) for each value of m separately, with $m=-n_c, -n_c+1, \dots, n_c-1, n_c$. For each m , Eq. (16) reduces to

$$\begin{pmatrix} \tilde{\mathcal{G}}^{(m)} & \bar{\mathcal{G}}^{(m)} \\ \tilde{\mathcal{E}}^{(m)} & \bar{\mathcal{E}}^{(m)} \end{pmatrix} \mathbf{c}^{(m)} = \lambda^{(m)} \mathbf{c}^{(m)}, \quad (47)$$

where $\tilde{\mathcal{G}}^{(m)},$ etc., are $n_d^{(m)} \times n_d^{(m)}$ matrices given by Eq. (17) with $u=m$ and $n, v=m_1, m_1+1, \dots, n_c$. Here,

$$n_d^{(m)} = n_c + 1 - m_1 \quad \text{with} \quad m_1 = \max(1, |m|). \quad (48)$$

The column vector $\mathbf{c}^{(m)}$ in Eq. (47) is

$$\begin{aligned} \mathbf{c}_v^{(m)} &= d_{mv}, \\ \mathbf{c}_{v+n_d^{(m)}}^{(m)} &= c_{mv} \end{aligned} \quad (49)$$

with $v=m_1, m_1+1, \dots, n_c$. The linear system (37) is simplified similarly so that $\Lambda^{(m)}, \bar{\Lambda}^{(m)},$ are $n_d^{(m)} \times n_d^{(m)}$ diagonal matrices, and $U^{(m)}, \bar{U}^{(m)}, V^{(m)}, \bar{V}^{(m)}$ are all $n_d^{(m)} \times 2n_d^{(m)}$ matrices. The calculation is much simplified by solving $2n_d^{(m)} \times 2n_d^{(m)}$ eigensystem and computing the inverse of $2n_d^{(m)} \times 2n_d^{(m)}$ matrix for each m , instead of dealing with matrices of much greater dimension n_t .

Further simplification can be made by taking advantage of the second Kronecker symbol $\delta_{n,v}, \delta_{n\pm 1,v},$ and $\delta_{n\pm 2,v}$ appearing in Eq. (10). Instead of solving the eigensystem (47), one can reorder the column vector $\mathbf{c}^{(m)}$ into $\mathbf{c}^{(m,\sigma)}$ given by

$$\mathbf{c}_v^{(m,\sigma)} = \begin{cases} d_{mv} & \text{if } v - m_1 \text{ is even} \\ c_{mv} & \text{if } v - m_1 \text{ is odd,} \end{cases} \quad (50)$$

$$\mathbf{c}_{v+n_d^{(m)}}^{(m,\sigma)} = \begin{cases} c_{mv} & \text{if } v - m_1 \text{ is even} \\ d_{mv} & \text{if } v - m_1 \text{ is odd,} \end{cases} \quad (51)$$

where, again, $v=m_1, m_1+1, \dots, n_c$. Let $\mathcal{T}^{(m)}$ denote the $2n_d^{(m)} \times 2n_d^{(m)}$ transformation matrix between $\mathbf{c}^{(m,\sigma)}$ and $\mathbf{c}^{(m)}$, i.e.,

$$\mathbf{c}^{(m,\sigma)} = \mathcal{T}^{(m)} \mathbf{c}^{(m)}. \quad (52)$$

After the transformation, the eigensystem (47) becomes

$$\mathcal{E} \mathbf{c}^{(m,\sigma)} = \lambda^{(m)} \mathbf{c}^{(m,\sigma)}, \quad (53)$$

where

$$\mathcal{E} = \mathcal{T}^{(m)} \begin{pmatrix} \tilde{\mathcal{G}}^{(m)} & \bar{\mathcal{G}}^{(m)} \\ \tilde{\mathcal{E}}^{(m)} & \bar{\mathcal{E}}^{(m)} \end{pmatrix} [\mathcal{T}^{(m)}]^{-1} \quad (54)$$

is of block-diagonal form and can be decomposed to two $n_d^{(m)} \times n_d^{(m)}$ submatrices. The same procedure applies to the linear system (37), resulting in the computation of the inverse of two $n_d^{(m)} \times n_d^{(m)}$ matrices instead of one $2n_d^{(m)} \times 2n_d^{(m)}$ matrix.

As a result, due to the axial symmetry of Eq. (1), one finally needs to solve a series of eigensystems and compute the inverse of a series of matrices. The dimension of these matrices are $n_d^{(m)} \times n_d^{(m)}$, with $n_d^{(m)}$ given by Eq. (48) and $m=-n_c, -n_c+1, \dots, n_c-1, n_c$. The maximum matrix dimension is limited to n_c , while solving Eqs. (16) and (41) directly requires operating with matrix of dimension $n_t=2n_c(n_c+2) \gg n_c$.

B. Evaluation of $S_n(x), T_n(x,z)$

Solution of Eq. (40) requires the evaluation of $S_n(x)$ and $T_n(x,z)$, etc., appearing in Eq. (38). To obtain reliable numerical values, $S_n(x)$ and $T_n(x,z)$ are evaluated based on the following recurrence relations:

$$S_n(x) = \frac{\xi_n(x)}{\psi_n(x)} = S_{n-1}(x) \frac{[D_n^{(1)}(x) + n/x]}{[D_n^{(3)}(x) + n/x]},$$

$$T_n(x,z) = \frac{\psi_n(z)}{\psi_n(x)} = T_{n-1}(x,z) \frac{[D_n^{(1)}(x) + n/x]}{[D_n^{(1)}(z) + n/z]}, \quad (55)$$

starting with the following initial values

$$S_0(x) = \frac{2e^{2ix}}{e^{2ix} - 1}, \quad (56a)$$

$$T_0(x,z) = \frac{e^{2iz} - 1}{e^{2ix} - 1} e^{i(x-z)}, \quad (56b)$$

for nonmetallic sphere. For metallic particle that has a large imaginary part in ϵ_s , on the other hand, the initial value (56b) can be replaced by

$$T_0(x, z) = \frac{e^{2iz} - 1}{e^{2ix} - 1} e^{ix} \quad (57)$$

to avoid numerical overflow, while the resultant α_l obtained from Eq. (40) for the internal fields have to be multiplied by $e^{m_l k_l x}$ accordingly. The remaining two quantities in Eq. (39), $\bar{S}_n(x)$ and $\bar{T}_n(x, z)$, are computed using

$$\begin{aligned} \bar{S}_n(x) &= \frac{\xi'_n(x)}{\psi'_n(x)} = S_n(x) \frac{D_n^{(3)}(x)}{D_n^{(1)}(x)}, \\ \bar{T}_n(x, z) &= \frac{\psi'_n(z)}{\psi'_n(x)} = T_n(x, z) \frac{D_n^{(1)}(z)}{D_n^{(1)}(x)}, \end{aligned} \quad (58)$$

where the logarithmic derivatives of the Riccati-Bessel functions are defined by

$$D_n^{(1)}(z) = \psi'_n(z)/\psi_n(z), \quad D_n^{(3)}(z) = \xi'_n(z)/\xi_n(z). \quad (59)$$

In our calculation, $D_n^{(1)}(z)$ is evaluated based on the downward recurrence relation [27]

$$D_{n-1}^{(1)}(z) = \frac{n}{z} - \frac{1}{D_n^{(1)}(z) + \frac{n}{z}} \quad (60)$$

starting from an asymptotic value $D_{n_{st}} = 0.0 + i0.0$ with $n_{st} = \max(|z|, n_c + 15)$. For $D_n^{(3)}(z)$, we found that a simple upward recurrence,

$$D_n^{(3)}(z) = -\frac{n}{z} + \frac{1}{\frac{n}{z} - D_{n-1}^{(3)}(z)}, \quad (61)$$

starting with $D_0^{(3)} = i$ yields results with a satisfactory numerical accuracy.

C. Effect of anisotropy

We are now ready to present some numerical examples demonstrating the effect of the anisotropy. Due to the anisotropy in the permeability, the scattering depends on the angle of incidence, denoted by θ_k as shown in Fig. 1, as well as the polarization of the incident wave. The axial symmetry of the permeability implies that the scattering is independent of the azimuthal angle ϕ_k . In this section, without loss of generality, we set $\phi_k = 0$, which implies $\hat{\phi}_k = \mathbf{e}_y$, and the efficiency of scattering $Q_{sca}(\theta_k)$ is a function of incident angle θ_k .

To concentrate on the effect of anisotropy solely, we study two simple matching cases. Case I is the uniaxially anisotropic particle with $\epsilon_s = \epsilon_0$ and

$$\vec{\mu} = \mu_0 \begin{pmatrix} 1 & 0 & 0 \\ 0 & 1 & 0 \\ 0 & 0 & 1 + u \end{pmatrix}, \quad (62)$$

such that the refractive indices of the particle and the surrounding medium are matched when the uniaxial anisotropy parameter $u = 0$. This case is called uniformly anisotropic in Ref. [25], with $u > 0$ and $u < 0$ corresponding, respectively,

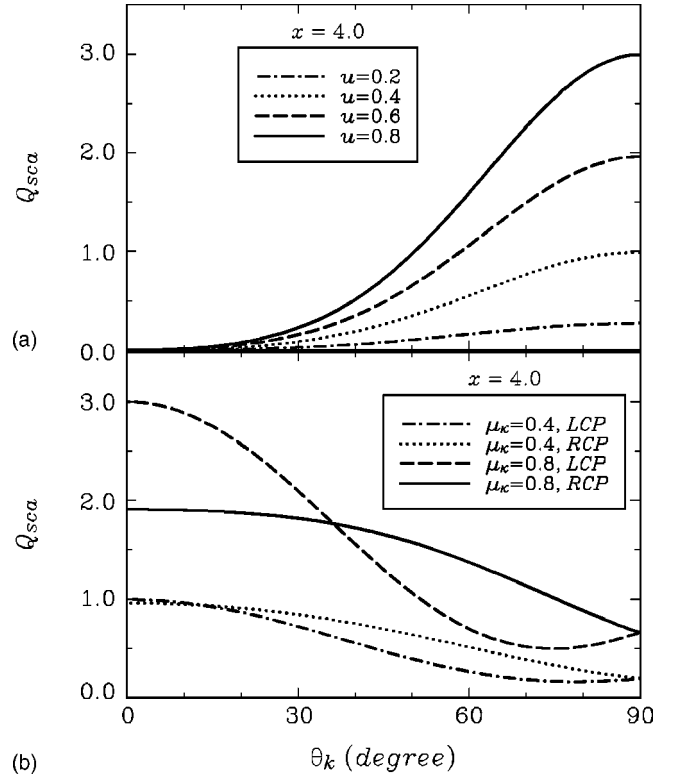


FIG. 2. (a) Scattering efficiency Q_{sca} as a function of incident angle θ_k for case I with the size parameter $x = k_0 r_s = 4.0$ at various values of u . The incident wave is linearly polarized with $(p_\theta, p_\phi) = (0, 1)$. (b) Scattering efficiency Q_{sca} as a function of θ_k for case II with $x = 4.0$ at various values of μ_κ . LCP and RCP denote the left and right circularly polarized incident waves, with $(p_\theta, p_\phi) = 1/\sqrt{2}(1, i)$ and $(p_\theta, p_\phi) = 1/\sqrt{2}(1, -i)$, respectively.

to positive and negative uniaxial particles. Case II is the gyromagnetic anisotropic particle with $\epsilon_s = \epsilon_0$ and

$$\vec{\mu} = \mu_0 \begin{pmatrix} 1 & -i\mu_\kappa & 0 \\ i\mu_\kappa & 1 & 0 \\ 0 & 0 & 1 \end{pmatrix}. \quad (63)$$

The refractive indices of particle and the surrounding medium are also matched if the gyromagnetic anisotropy parameter $\mu_\kappa = 0$. In both cases, the scattering is due solely to the anisotropy, differing from those where the isotropic optical contrast dominates [27].

For case I, it is noted that the y component of \mathbf{H} field of the incident wave is not affected by the scatterer [25], leading to a vanishing scattering efficiency for an incident wave with $(p_\theta, p_\phi) = (1, 0)$ [see Eq. (26)]. So for case I, we limit to the scattering of the incident plane wave with linear polarization given by $(p_\theta, p_\phi) = (0, 1)$. For case II, on the other hand, we focus on the circularly polarized incident wave, with $(p_\theta, p_\phi) = 1/\sqrt{2}(1, i)$ and $(p_\theta, p_\phi) = 1/\sqrt{2}(1, -i)$, corresponding, respectively, to left circular polarization (LCP) and right circular polarization (RCP).

The dependences of the scattering efficiency on the incident angle is shown in Fig. 2 for cases I and II, at different values of u and μ_κ . It is found that if the size parameter x is

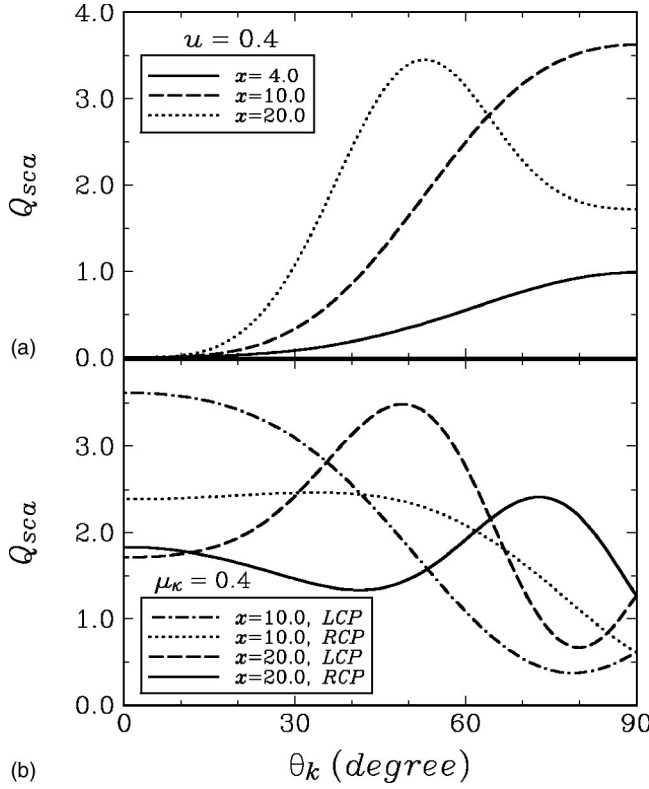


FIG. 3. (a) The same as Fig. 2(a), with $u=0.4$ at various values of the size parameter x . (b) The same as Fig. 2(b), with $\mu_\kappa=0.4$ at various values of x .

not very large, the scattering efficiency Q_{sca} for case I monotonically increases with the incident angle θ_k in the region from 0 to $\pi/2$, while it decreases with θ_k in the region from $\pi/2$ to π due to symmetry $Q_{sca}(\theta_k) = Q_{sca}(\pi - \theta_k)$. For case II, on the other hand, Q_{sca} decreases with the θ_k for $0 \leq \theta_k \leq \pi/2$ for small μ_κ , whereas it increases for $(\pi/2) \leq \theta_k \leq \pi$ owing to the symmetry $Q_{sca}^\sigma(\theta_k) = Q_{sca}^{-\sigma}(\pi - \theta_k)$. Here $\sigma = \pm 1$, with $\sigma = +1$ ($\sigma = -1$) denoting the incident wave of LCP (RCP). For bigger μ_κ , the dependence on θ_k is no longer monotonical, as shown in Fig. 2(b) for $\mu_\kappa=0.8$ and LCP incidence.

Figure 3 shows Q_{sca} versus θ_k for different values of the size parameter x , with $u=0.4$ for case I and $\mu_\kappa=0.4$ for case II. It is seen that the dependence on θ_k is no longer monotonic for relatively large x . For $x=20$, e.g., Q_{sca} reaches maximum at $\theta_k=53^\circ$ for case I, and at $\theta_k=49^\circ$, and 73° for case II with LCP and RCP incidence, respectively.

$Q_{sca}(0)$ versus x for case II with $\mu_\kappa=0.4$ exhibits oscillatory behavior as shown in Fig. 4 for both LCP and RCP incidences. $Q_{sca}(\pi/2)$ versus x for case I with $u=0.4$ ($u=-0.4$) is found coincide with $Q_{sca}^{LCP}(0)$ versus x [$Q_{sca}^{RCP}(0)$ versus x] for case II with $\mu_\kappa=0.4$. The reasons for these coincidences are as follows. For case II with $\theta_k=0$, the effective permeability for incident wave of LCP (RCP) is, for $\mu_\kappa=0.4$, $\mu_{eff}^{LCP} = (1 + \mu_\kappa)\mu_0 = 1.4\mu_0$, [$\mu_{eff}^{RCP} = (1 - \mu_\kappa)\mu_0 = 0.6\mu_0$], as inferred from Eq. (63). For case I with $\theta_k = \pi/2$ and \mathbf{H}_{inc} polarized in z direction [corresponding to $(p_\theta, p_\phi) = (0, 1)$], the effective permeability is $\mu_{eff}^{Hz} = \mu_s = (1 + u)\mu_0 = 1.4\mu_0$ and $0.6\mu_0$ for $u=0.4$ and -0.4 , respectively.

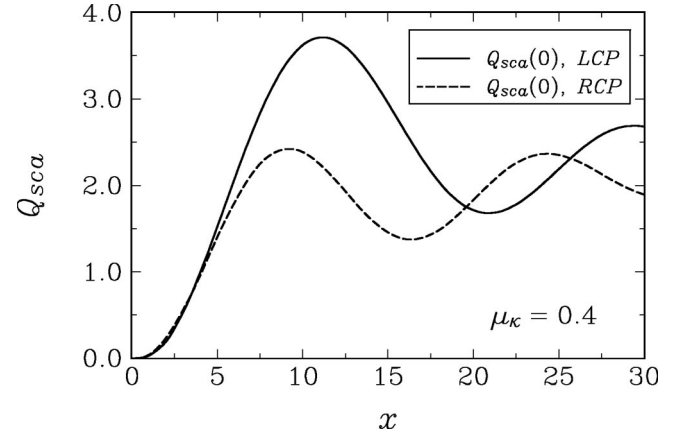


FIG. 4. Scattering efficiency $Q_{sca}(0)$ vs the size parameter x for case II with $\mu_\kappa=0.4$. LCP and RCP denoting, respectively, left and right circularly polarized incident waves.

This leads to the coincident overlap of the Q_{sca} versus x curves. Such coincident overlap of the Q_{sca} versus x curves is found to be unique for matching cases in which the scattering is due solely to the optical anisotropy. For the mismatching case with isotropic optical contrast between the particle and surrounding medium, no such coincidence behavior is observed.

$Q_{sca}(\pi/2)$ [$Q_{sca}(0)$] as a function of u (μ_κ) is shown in Fig. 5(a) [Fig. 5(b)] for case I (case II) with $-0.4 \leq u \leq 1.0$ ($0 \leq \mu_\kappa \leq 0.8$), at different values of x . Different oscillatory behaviors are observed for large x , leading to the appearance of peaks in the range of u (μ_κ) studied.

D. Photonic Hall effect

We now turn to more general scattering problems. Of particular interest is the so-called photonic Hall effect, a manifestation of a magnetic field induced transverse current in the light transport, which bears a strong phenomenological resemblance to the electronic Hall effect. The photonic Hall effect finds its origin in the magnetically induced changes of the optical parameters. Based on perturbation theory, Lacoste *et al.* [20] have addressed the issue whether or not there is a photonic Hall effect for one single Mie scatterer. Here, as the second numerical example, we present our results based on the exact Mie-type solution [30].

Figure 6 is a polar plot of the magnetotransverse scattering cross section $F(\theta, \phi)$ at $\theta = \pi/2$, for the case with size parameter $x=3$, $\epsilon_s = \epsilon_0$, $\mu_s = 1.5\mu_0$, $\mu_r = 1$, and $\mu_\kappa = 0.001$ [Fig. 6(a)], $\mu_\kappa = 0.01$ [Fig. 6(b)]. Here θ (ϕ) denotes the polar (azimuthal) angle of \mathbf{r} . The incident wave vector is in x direction, given by $\theta_k = \pi/2$ and $\phi_k = 0$, and normal to the direction of the applied magnetic field in z direction. This corresponds to the maximum effect of the transverse scattering [20]. The magnetotransverse scattering cross section $F(\theta, \phi)$ is defined by the difference of differential scattering cross sections for the cases with $\mu_\kappa \neq 0$ and $\mu_\kappa = 0$, corresponding to the cases in the presence and in the absence of the externally applied magnetic field, respectively [30].

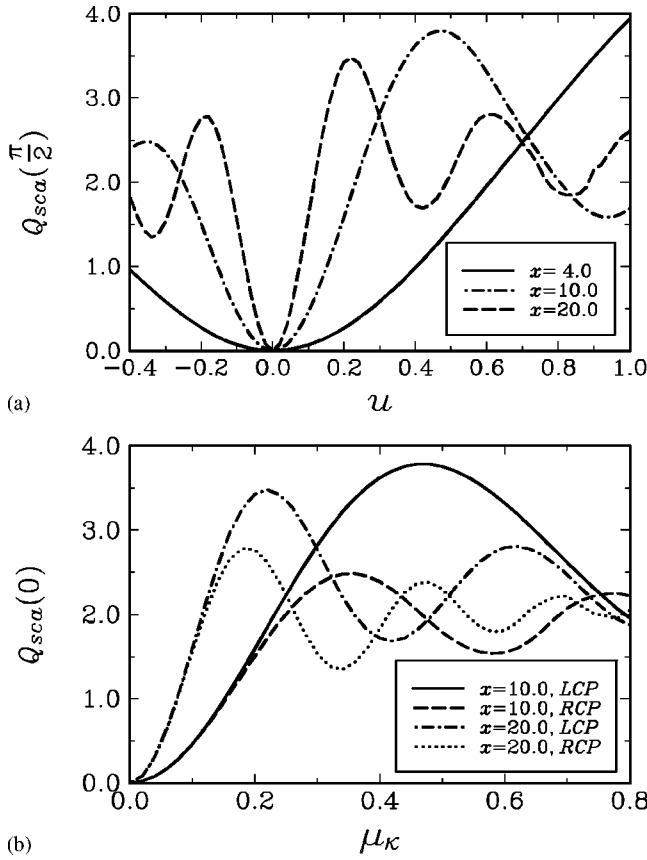


FIG. 5. (a) Scattering efficiency $Q_{\text{sca}}(\pi/2)$ vs u for case I at various values of the size parameter x . The incident wave is linearly polarized with $(p_\theta, p_\phi) = (0, 1)$. (b) Scattering efficiency $Q_{\text{sca}}(0)$ vs μ_κ for case II at various values of x . The incident wave is either left or right circularly polarized, denoted by LCP and RCP, with $(p_\theta, p_\phi) = 1/\sqrt{2}(1, i)$ and $1/\sqrt{2}(1, -i)$, respectively.

$$F(\theta, \phi) = \left. \frac{d\sigma(\theta, \phi)}{d\Omega} \right|_{\mu_\kappa \neq 0} - \left. \frac{d\sigma(\theta, \phi)}{d\Omega} \right|_{\mu_\kappa = 0}. \quad (64)$$

The differential scattering cross section is given by

$$\frac{d\sigma(\theta, \phi)}{d\Omega} = |\mathbf{f}(\theta, \phi)|^2 \quad (65)$$

with the scattering amplitude $\mathbf{f}(\theta, \phi)$ defined by

$$\mathbf{E}_s = E_0 \mathbf{f}(\theta, \phi) \frac{e^{ik_0 r}}{r}, \quad r = |\mathbf{r}| \rightarrow \infty. \quad (66)$$

From Fig. 6, it is seen that a net magnetotransverse scattering is expected because the projections onto the y axis of $F(\theta, \phi)$ do not cancel, confirming the possibility of photonic Hall effect for a single Mie scatterer [20]. In addition, it is found that for small μ_κ , $F(\pi/2, 2\pi - \phi) = -F(\pi/2, \phi)$, exhibiting antisymmetry with respect to the incident direction, in agreement with the results based on the perturbation approach [20]. For bigger μ_κ , the antisymmetry is ruined, as displayed in Fig. 6(b), suggesting the possible failure of the perturbation theory.

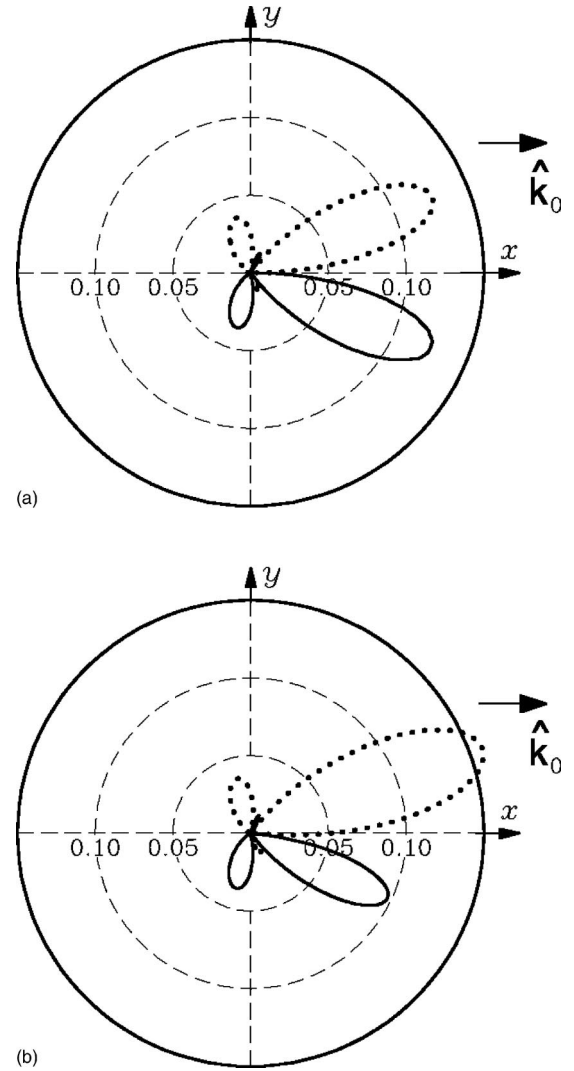


FIG. 6. Polar plot of magnetotransverse cross section $F(\theta, \phi)$ at $\theta = \pi/2$ for a Mie scatterer of size parameter $x = 3$ with $\mu_\kappa = 0.001$ (a) and $\mu_\kappa = 0.01$ (b). The curves have been normalized by μ_κ . Solid line (dotted line) denotes positive (negative) values for $F(\theta, \phi)$. The applied magnetic field is in z direction (normal to the plot) and incident wave vector in x direction. A net magnetotransverse scattering is expected for both cases, because the projections onto y axis of $F(\theta, \phi)$ do not cancel. For bigger μ_κ , the antisymmetry $F(\pi/2, \phi) = -F(\pi/2, 2\pi - \phi)$ is ruined.

To quantitatively describe the anisotropy of light scattering, one usually associates the transverse light current I with an integration of magnetotransverse scattering cross section $F(\theta, \phi)$ over outgoing wave vectors,

$$I = \int_0^\pi \sin \theta d\theta \int_0^{2\pi} d\phi F(\theta, \phi) \sin \theta \sin \phi, \quad (67)$$

where the factor $\sin \theta \sin \phi$ represents a projection onto the magnetotransverse direction, which is the y direction if we assume that the applied external \mathbf{B}_0 field is in z direction and the incident wave vector is in x direction. Lacoste [20] proposed to normalize I by the total transverse light current when $\mu_\kappa = 0$ (corresponding to the case in the absence of

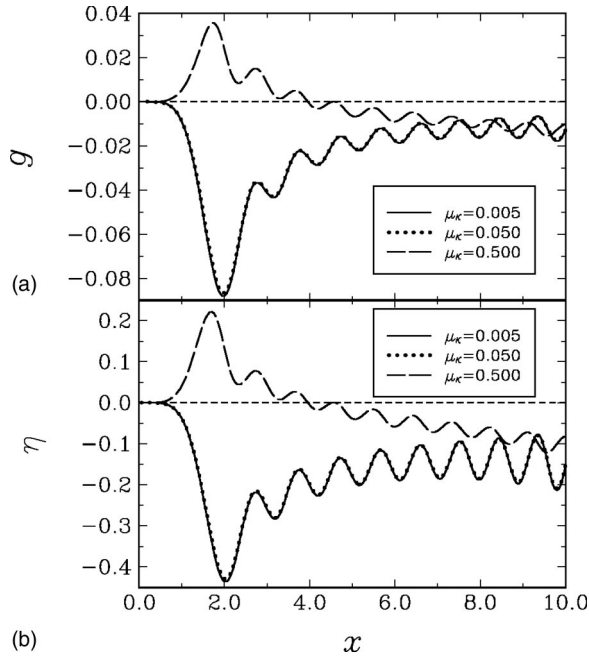


FIG. 7. Asymmetry parameter g (a) and normalized magnetotransverse light current η vs the size parameter $x = k_0 r_s$ at various values of μ_κ . The curves have been normalized by μ_κ . Results for $\mu_\kappa = 0.005$ and $\mu_\kappa = 0.05$ show no graphically discernible difference, suggesting the linear dependence of η on μ_κ and thus on the externally applied \mathbf{B}_0 field. For bigger μ_κ , the dependence of η on μ_κ is no longer linear. In addition, a change of sign in η is observed.

applied magnetic field \mathbf{B}_0) [30], which leads to

$$\eta = \frac{I}{\int_0^\pi \sin \theta d\theta \int_0^{2\pi} d\phi |\mathbf{f}(\theta, \phi)|^2 |\sin \theta \sin \phi|}. \quad (68)$$

If one chooses a coordinate system such that the applied \mathbf{B}_0 field is in the x direction and incident wave is along the y direction, then the transverse light current \mathbf{I} becomes

$$\mathbf{I} = g C_{sca} \quad (69)$$

with the asymmetry parameter g given by Eq. (42d). When normalized by the total scattering cross section, the transverse light current reduces actually to the asymmetry parameter g that is readily available from Eq. (42d), avoiding the integration over outgoing wave vectors (68).

Figure 7 shows both η and g as a function of the size parameter x for the case with $\epsilon_s = \epsilon_0$, $\mu_s = 1.5\mu_0$, $\mu_r = 1.0$, and different values of μ_κ . The transverse light current due to nonvanishing μ_κ is clearly observed, confirming the possibility of a photonic Hall effect for a single Mie scatterer. It is also noted that, when normalized by μ_κ , the results for $\mu_\kappa = 0.005$ and $\mu_\kappa = 0.05$ show no graphically discernible difference, suggesting the linear dependence of η on μ_κ , in agreement with the linear magnetic field dependence of the magnetotransverse photon flux [13–17,30]. When μ_κ is big enough, the linear dependence is found to be ruined. In addition, a change of sign in η is observed at certain x that depends on the value of μ_κ .

IV. SUMMARY

We have extended the Mie theory for electromagnetic scattering by spherical particle to the case of a magnetic particle that possesses the gyromagnetic form of permeability (1), which includes the uniaxial anisotropy as a special case. This is done by first constructing for the magnetic induction \mathbf{B}_I inside the particle a new set of vector basis functions in terms of the usual VSWF's with different values of wave vector k_l . The values of k_l are the eigenvalues of an eigensystem determined by the permeability tensor. The new set of vector basis functions are divergenceless and satisfy the wave equation for \mathbf{B}_I . With the \mathbf{B}_I field expanded in terms of the new set of vector basis functions (21), \mathbf{E}_I and \mathbf{H}_I fields can then be written based on VSWF's with the different values of wave vector k_l , instead of a single value in isotropic case. The difference from isotropic sphere lies also in that the expansion of \mathbf{H}_I field includes the third set of VSWF's \mathbf{L}_{mn} in addition to the usual \mathbf{M}_{mn} and \mathbf{N}_{mn} , because \mathbf{H}_I is no longer divergenceless. The incident and scattered fields are expanded as usual in terms of the VSWF's. By matching the boundary conditions, a linear set of coupled equations for the expansion coefficients are obtained and then solved for the solution to the scattering problem.

The formulation can be applied to the case with arbitrarily anisotropic permeability tensor $\tilde{\mu}$, provided that the expansion coefficients of $\tilde{\mu}^{-1} \cdot \mathbf{M}_{mn}$ and $\tilde{\mu}^{-1} \cdot \mathbf{N}_{mn}$ in terms of VSWF's such as Eq. (9) can be worked out. The particular axial symmetry of Eq. (1) greatly reduces numerical complexity and thus avoids numerical errors in dealing with matrices of large dimensions.

As the first application of the formulation, we present some numerical results for scattering due solely to the optical anisotropy within the particle. The scattering efficiency exhibits miscellaneous dependence behaviors on the incident angle, the polarization, the anisotropy parameter, as well as the size parameter. In the second example, we study the transverse electromagnetic scattering effect. Our results confirm the possibility of the photonic Hall effect for one single Mie scatterer.

Apart from magnetic particles, the formulation presented here is also expected to find applications in electromagnetic scattering by plasma sphere in external dc magnetic field, with some minor revisions to take into account the gyroelectric characteristics.

ACKNOWLEDGMENTS

Z.L. wishes to thank Professor C. T. Chan for helpful discussion. Z.L. was supported in part by CNKBRF and CUNSF. S.T.C. was supported by DARPA and the NSF.

APPENDIX A: VECTOR SPHERICAL WAVE FUNCTIONS

The VSWF's $\mathbf{M}_{mn}^{(j)}$, $\mathbf{N}_{mn}^{(j)}$, and $\mathbf{L}_{mn}^{(j)}$ are given by [24,26]

$$\mathbf{M}_{mn}^{(j)}(k, \mathbf{r}) = [i\pi_{nm}(\cos \theta)\mathbf{e}_\theta - \tau_{nm}(\cos \theta)\mathbf{e}_\phi] z_n^{(j)}(kr) e^{im\phi},$$

$$\begin{aligned} \mathbf{N}_{mn}^{(J)}(k, \mathbf{r}) &= [\tau_{mn}(\cos \theta) \mathbf{e}_\theta + i\pi_{mn}(\cos \theta) \mathbf{e}_\phi] \frac{1}{kr} \frac{d}{dr} [rz_n^{(J)}(kr)] \\ &\quad \times e^{im\phi} + \mathbf{e}_r n(n+1) P_n^m(\cos \theta) \frac{z_n^{(J)}(kr)}{kr} e^{im\phi}, \\ \mathbf{L}_{mn}^{(J)}(k, \mathbf{r}) &= [\tau_{mn}(\cos \theta) \mathbf{e}_\theta + i\pi_{mn}(\cos \theta) \mathbf{e}_\phi] \frac{z_n^{(J)}(kr)}{kr} e^{im\phi} \\ &\quad + \mathbf{e}_r P_n^m(\cos \theta) \frac{1}{k} \frac{d}{dr} [z_n^{(J)}(kr)] e^{im\phi}, \end{aligned} \quad (\text{A1})$$

where \mathbf{e}_r , \mathbf{e}_θ , and \mathbf{e}_ϕ are three unit base vectors in spherical coordinate system, and $P_n^m(x)$ is the first kind associated Legendre function [26,27]. The radial function $z_n^{(J)}$ is given by

$$z_n^{(1)}(x) = j_n(x), z_n^{(3)}(x) = h_n^{(1)}(x) \quad (\text{A2})$$

with $j_n(x)$ the first kind of spherical Bessel function and $h_n^{(1)}(x)$ the first kind spherical Hankel functions. Two auxiliary functions, $\pi_{mn}(\cos \theta)$ and $\tau_{mn}(\cos \theta)$, are defined by

$$\begin{aligned} \pi_{mn}(\cos \theta) &= \frac{m}{\sin \theta} P_n^m(\cos \theta), \\ \tau_{mn}(\cos \theta) &= \frac{d}{d\theta} P_n^m(\cos \theta). \end{aligned} \quad (\text{A3})$$

The VSWF's satisfy

$$\nabla \times \nabla \times \mathbf{M}_{mn}^{(J)} - k^2 \mathbf{M}_{mn}^{(J)} = 0, \quad (\text{A4a})$$

$$\nabla \times \nabla \times \mathbf{N}_{mn}^{(J)} - k^2 \mathbf{N}_{mn}^{(J)} = 0,$$

$$\mathbf{M}_{mn}^{(J)} = \frac{1}{k} \nabla \times \mathbf{N}_{mn}^{(J)}, \mathbf{M}_{mn}^{(J)} = \frac{1}{k} \nabla \times \mathbf{N}_{mn}^{(J)}, \quad (\text{A4b})$$

$$\nabla \cdot \mathbf{M}_{mn}^{(J)} = 0, \nabla \cdot \mathbf{N}_{mn}^{(J)} = 0, \nabla \times \mathbf{L}_{mn}^{(J)} = 0. \quad (\text{A4c})$$

They are orthogonal in the sense that [26],

$$\int_0^{2\pi} \int_0^\pi \mathbf{M}_{uv}^* \cdot \mathbf{N}_{mn} \sin \theta d\theta d\phi = 0,$$

$$\int_0^{2\pi} \int_0^\pi \mathbf{L}_{uv}^* \cdot \mathbf{M}_{mn} \sin \theta d\theta d\phi = 0,$$

$$\begin{aligned} &\int_0^{2\pi} \int_0^\pi \mathbf{M}_{uv}^* \cdot \mathbf{M}_{mn} \sin \theta d\theta d\phi \\ &= \frac{4\pi n(n+1)}{2n+1} \frac{(n+m)!}{(n-m)!} z_n^2(kr) \delta_{mu} \delta_{nv}, \end{aligned}$$

$$\begin{aligned} &\int_0^{2\pi} \int_0^\pi \mathbf{N}_{uv}^* \cdot \mathbf{N}_{mn} \sin \theta d\theta d\phi \\ &= \frac{4\pi n(n+1)}{(2n+1)^2} \frac{(n+m)!}{(n-m)!} \\ &\quad \times [(n+1)z_{n-1}^2(kr) + nz_{n+1}^2(kr)] \delta_{mu} \delta_{nv}, \end{aligned}$$

$$\begin{aligned} &\int_0^{2\pi} \int_0^\pi \mathbf{L}_{uv}^* \cdot \mathbf{L}_{mn} \sin \theta d\theta d\phi \\ &= \frac{4\pi}{(2n+1)^2} \frac{(n+m)!}{(n-m)!} [nz_{n-1}^2(kr) + (n+1)z_{n+1}^2(kr)] \delta_{mu} \delta_{nv}, \end{aligned}$$

$$\begin{aligned} &\int_0^{2\pi} \int_0^\pi \mathbf{L}_{uv}^* \cdot \mathbf{N}_{mn} \sin \theta d\theta d\phi \\ &= \frac{4\pi n(n+1)}{(2n+1)^2} \frac{(n+m)!}{(n-m)!} [z_{n-1}^2(kr) - z_{n+1}^2(kr)] \delta_{mu} \delta_{nv}, \end{aligned} \quad (\text{A5})$$

where the superscript \star denotes the complex conjugate on angular functions, differing from the superscript $*$ that stands for the complete complex conjugate, e.g.,

$$\mathbf{M}_{mn}(k, \mathbf{r}) = [i\pi_{mn}(\cos \theta) \mathbf{e}_\theta - \tau_{mn}(\cos \theta) \mathbf{e}_\phi] z_n(kr) e^{im\phi},$$

$$\mathbf{M}_{mn}^*(k, \mathbf{r}) = [-i\pi_{mn}(\cos \theta) \mathbf{e}_\theta - \tau_{mn}(\cos \theta) \mathbf{e}_\phi] z_n(kr) e^{-im\phi},$$

$$\mathbf{M}_{mn}^*(k, \mathbf{r}) = [-i\pi_{mn}(\cos \theta) \mathbf{e}_\theta - \tau_{mn}(\cos \theta) \mathbf{e}_\phi] z_n^*(kr) e^{-im\phi}.$$

APPENDIX B: EXPANSION OF $\vec{\mu}^{-1} \cdot \mathbf{M}_{mn}$ and $\vec{\mu}^{-1} \cdot \mathbf{N}_{mn}$

In this appendix, we outline the derivation of the expansions (9) for $\vec{\mu}^{-1} \cdot \mathbf{M}_{mn}$ and $\vec{\mu}^{-1} \cdot \mathbf{N}_{mn}$. In dyadic form, Eq. (5) can be rewritten as

$$\begin{aligned} \mu_s \vec{\mu}^{-1} &= \mu'_r \mathbf{e}_x \mathbf{e}_x - i\mu'_\kappa \mathbf{e}_x \mathbf{e}_y + i\mu'_\kappa \mathbf{e}_y \mathbf{e}_x + \mu'_r \mathbf{e}_y \mathbf{e}_y + \mathbf{e}_z \mathbf{e}_z \\ &= \mu'_+ \mathbf{e}_+ \mathbf{e}_+ + \mu'_- \mathbf{e}_- \mathbf{e}_- + \mathbf{e}_0 \mathbf{e}_0, \end{aligned} \quad (\text{B1})$$

where the superscript $*$ denotes, as usual, the complex conjugate,

$$\mathbf{e}_+ = \frac{1}{\sqrt{2}} (\mathbf{e}_x + i\mathbf{e}_y),$$

$$\mathbf{e}_0 = \mathbf{e}_z,$$

$$\mathbf{e}_- = \frac{1}{\sqrt{2}} (\mathbf{e}_x - i\mathbf{e}_y), \quad (\text{B2})$$

and $\mu'_\pm = \mu'_r \mp i\mu'_\kappa$. Rewritten in terms of \mathbf{e}_\pm and \mathbf{e}_0 the VSWF's Eq. (A1) become

$$\begin{aligned} \mathbf{M}_{mn}^{(J)}(k, \mathbf{r}) &= \frac{i}{\sqrt{2}}(n+m)(n-m+1)X_n^{m-1}z_n^{(J)}\mathbf{e}_-^* \\ &+ \frac{i}{\sqrt{2}}X_n^{m+1}z_n^{(J)}\mathbf{e}_+^* - imX_n^m z_n^{(J)}\mathbf{e}_0, \end{aligned} \quad (\text{B3a})$$

$$\begin{aligned} \mathbf{N}_{mn}^{(J)}(k, \mathbf{r}) &= \frac{1}{\sqrt{2}} \left[\frac{(n+1)(n+m)(n+m-1)}{2n+1} X_{n-1}^{m-1} z_{n-1}^{(J)} \right. \\ &- \left. \frac{n(n-m+1)(n-m+2)}{2n+1} X_{n+1}^{m-1} z_{n+1}^{(J)} \right] \mathbf{e}_-^* \\ &+ \frac{1}{\sqrt{2}(2n+1)} [nX_{n+1}^{m+1} z_{n+1}^{(J)} - (n+1)X_{n-1}^{m+1} z_{n-1}^{(J)}] \mathbf{e}_+^* \\ &+ \left[\frac{n(n-m+1)}{2n+1} X_{n+1}^m z_{n+1}^{(J)} \right. \\ &+ \left. \frac{(n+1)(n+m)}{2n+1} X_{n-1}^m z_{n-1}^{(J)} \right] \mathbf{e}_0, \end{aligned} \quad (\text{B3b})$$

$$\begin{aligned} \mathbf{L}_{mn}^{(J)}(k, \mathbf{r}) &= \frac{1}{\sqrt{2}} \left[\frac{(n+m)(n+m-1)}{2n+1} X_{n-1}^{m-1} z_{n-1}^{(J)} \right. \\ &+ \left. \frac{(n-m+1)(n-m+2)}{2n+1} X_{n+1}^{m-1} z_{n+1}^{(J)} \right] \mathbf{e}_-^* \\ &- \frac{1}{\sqrt{2}(2n+1)} [X_{n+1}^{m+1} z_{n+1}^{(J)} + X_{n-1}^{m+1} z_{n-1}^{(J)}] \mathbf{e}_+^* \\ &- \left[\frac{(n-m+1)}{2n+1} X_{n+1}^m z_{n+1}^{(J)} - \frac{(n+m)}{2n+1} X_{n-1}^m z_{n-1}^{(J)} \right] \mathbf{e}_0 \end{aligned} \quad (\text{B3c})$$

with $X_n^m = P_n^m(\cos \theta) e^{im\phi}$ satisfying

$$\int_0^{2\pi} \int_0^\pi \bar{X}_v^u X_n^m \sin \theta d\theta d\phi = \frac{4\pi}{2n+1} \frac{(n+m)!}{(n-m)!} \delta_{nv} \delta_{mu}, \quad (\text{B4})$$

where $\bar{X}_v^u = P_v^u(\cos \theta) e^{-iu\phi}$. Multiplying (B3a) by dyad $\mu_s \tilde{\mu}^{-1}$ gives

$$\begin{aligned} \mu_s \tilde{\mu}^{-1} \cdot \mathbf{M}_{mn} &= \frac{i}{\sqrt{2}}(n+m)(n-m+1)\mu'_- X_n^{m-1} z_n \mathbf{e}_-^* \\ &+ \frac{i}{\sqrt{2}}\mu'_+ X_n^{m+1} z_n \mathbf{e}_+^* - imX_n^m z_n \mathbf{e}_0 \\ &= \sum_{q=0}^{+\infty} \sum_{p=-q}^{+q} [\tilde{g}_{pq}^{mn} \mathbf{M}_{pq} + \tilde{e}_{pq}^{mn} \mathbf{N}_{pq} + \tilde{f}_{pq}^{mn} \mathbf{L}_{pq}], \end{aligned} \quad (\text{B5})$$

where use has been made of Eq. (B1) and the second equality follows from the expansion of any vector field in terms of the VSWF's. Taking the scalar product of Eq. (B5) with \mathbf{M}_{uv}^* given by

$$\begin{aligned} \mathbf{M}_{uv}^*(k, \mathbf{r}) &= -\frac{i}{\sqrt{2}}(v+u)(v-u+1)\bar{X}_v^{u-1} z_v(kr) \mathbf{e}_- \\ &- \frac{i}{\sqrt{2}}\bar{X}_v^{u+1} z_v(kr) \mathbf{e}_+ + iu\bar{X}_v^u z_v(kr) \mathbf{e}_0 \end{aligned} \quad (\text{B6})$$

leads to

$$\begin{aligned} \sum_{q=0}^{+\infty} \sum_{p=-q}^{+q} \mathbf{M}_{uv}^* \cdot [\tilde{g}_{pq}^{mn} \mathbf{M}_{pq} + \tilde{e}_{pq}^{mn} \mathbf{N}_{pq} + \tilde{f}_{pq}^{mn} \mathbf{L}_{pq}] \\ = \left[\frac{\gamma}{2} \mu'_- X_n^{m-1} \bar{X}_v^{u-1} + \frac{1}{2} \mu'_+ X_n^{m+1} \bar{X}_v^{u+1} + mu X_n^m \bar{X}_v^u \right] z_n z_v \end{aligned} \quad (\text{B7})$$

with $\gamma = (n+m)(n-m+1)(v+u)(v-u+1)$. Integrating both sides of Eq. (B7) over the solid angle and taking into account the orthogonality relations (A5) and (B4) yield Eq. (10a). Similarly, taking the dot product of Eq. (B5) with \mathbf{N}_{uv}^* and \mathbf{L}_{uv}^* , respectively, and integrating over solid angle results in two linear equations, which can be easily solved to give Eqs. (10b) and (10c).

In a similar way, by taking the posterior scalar product of dyad $\mu_s \tilde{\mu}^{-1}$ and vector \mathbf{N}_{mn} given by Eq. (B3b) and expanding the resulting vector $\mu_s \tilde{\mu}^{-1} \cdot \mathbf{N}_{mn}$ in terms of the VSWF's, one gets an equation analogous to Eq. (B5). Taking the scalar product of this equation with \mathbf{M}_{uv}^* , \mathbf{N}_{uv}^* , and \mathbf{L}_{uv}^* , respectively, and integrating over solid angle give rise to three linear equations, which can be solved to produce Eqs. (10d)–(10f).

-
- [1] J. B. Pendry, Phys. Rev. Lett. **85**, 3966 (2000).
[2] R. A. Shelby, D. R. Smith, and S. Schultz, Science **292**, 77 (2001).
[3] D. R. Smith and D. Schurig, Phys. Rev. Lett. **90**, 077405 (2003).
[4] J. Li, L. Zhou, C. T. Chan, and P. Sheng, Phys. Rev. Lett. **90**, 083901 (2003).
[5] J. B. Pendry, Opt. Express **11**(7) (2003), and references therein, special issue on Negative Refraction and Metamaterials.

- [6] D. R. Smith, *Left-handed Materials Home*, http://physics.ucsd.edu/~drsleft_home.htm
[7] S. T. Chui and L. B. Hu, Phys. Rev. B **65**, 144407 (2002).
[8] S. T. Chui, Z. F. Lin, and L. B. Hu, Phys. Lett. A **319**, 85 (2003).
[9] M. M. Sigalas, C. M. Soukoulis, R. Biswas, and K. M. Ho, Phys. Rev. B **56**, 959 (1997).
[10] A. Moroz, Phys. Rev. B **66**, 115109 (2002).
[11] B. A. van Tiggellen and G. L. J. A. Rikken, in *Optical Properties of Nanostructured Random Media*, edited by V. M.

- Shalaev (Springer, Berlin, 2002), p. 275, and references therein.
- [12] F. A. Erbacher, R. Lenke, and G. Maret, *Europhys. Lett.* **21**, 551 (1993).
- [13] B. A. van Tiggelen, *Phys. Rev. Lett.* **75**, 422 (1995).
- [14] G. L. J. A. Rikken and B. A. van Tiggelen, *Nature (London)* **38**, 54 (1996).
- [15] A. Sparenberg, G. L. J. A. Rikken, and B. A. van Tiggelen, *Phys. Rev. Lett.* **79**, 757 (1997).
- [16] G. L. J. A. Rikken, A. Sparenberg, and B. A. van Tiggelen, *Physica B* **246-247**, 188 (1998).
- [17] S. Wiebel, A. Sparenberg, G. L. J. A. Rikken, D. Lacoste, and B. A. van Tiggelen, *Phys. Rev. E* **62**, 8636 (2000).
- [18] F. C. MacKintosh and S. John, *Phys. Rev. B* **37**, 1884 (1988).
- [19] B. A. van Tiggelen, R. Maynard, and T. M. Nieuwenhuizen, *Phys. Rev. E* **53**, 2881 (1996).
- [20] D. Lacoste, B. A. van Tiggelen, G. L. J. A. Rikken, and A. Sparenberg, *J. Opt. Soc. Am. A* **15**, 1636 (1998).
- [21] D. Lacoste and B. A. van Tiggelen, *Phys. Rev. E* **61**, 4556 (2000).
- [22] *Light Scattering by Nonspherical Particles*, edited by M. I. Mishchenko, J. W. Hovenier, and L. D. Travis (Academic Press, New York, 2000).
- [23] M. I. Mishchenko, L. D. Travis, and A. Macke, in *Light Scattering by Nonspherical Particles* [22] Chap. 6.
- [24] Y. L. Xu, *Appl. Opt.* **34**, 4573 (1995); **36**, 9496 (1997); *Phys. Lett. A* **249**, 30 (1998); *Phys. Rev. E* **67**, 046620 (2003); *J. Opt. Soc. Am. A* **20**, 2093 (2003).
- [25] A. D. Kiselev, V. Y. Reshetnyak, and T. J. Sluckin, *Phys. Rev. E* **65**, 056609 (2002).
- [26] J. A. Stratton, *Electromagnetic Theory* (McGraw-Hill, New York, 1941).
- [27] C. F. Bohren and D. R. Huffman, *Absorption and Scattering of Light by Small Particles* (Wiley, New York, 1983).
- [28] L. Tsang, J. A. Kong, and R. T. Shin, *Theory of Microwave Remote Sensing* (Wiley, New York, 1985).
- [29] W. J. Wiscombe, *Appl. Opt.* **19**, 1505 (1980).
- [30] Actually, the applied magnetic field \mathbf{B}_0 leads to, up to first order in \mathbf{B}_0 , a gyroelectric form of electric permittivity while keeping magnetic permeability unchanged (and matching to the surrounding medium) [13–17]. Due to the duality principle, here we present, equivalently, results for the case with gyro-magnetic form of permeability while keep permittivity matching to the surrounding medium.